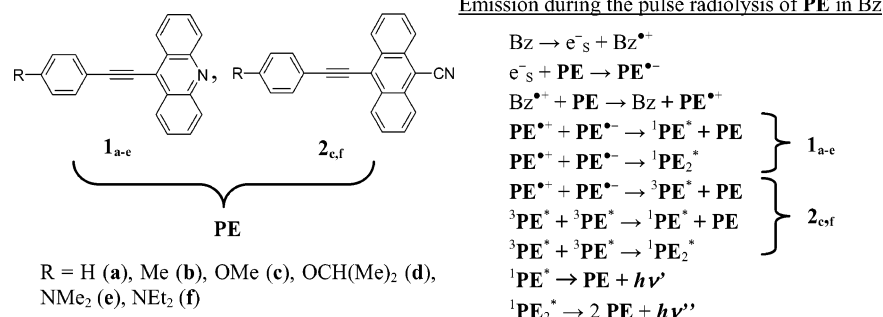# Efficient Emission from Charge Recombination during the Pulse Radiolysis of Electrochemical Luminescent Donor−Acceptor Molecules with an Ethynyl Linkage

Shingo Samori, Sachiko Tojo, Mamoru Fujitsuka, Shu-Wen Yang,[†] Arumugasamy Elangovan,[†] Tong-Ing Ho,[†] and Tetsuro Majima*

The Institute of Scientific and Industrial Research (SANKEN), Osaka University, Mihogaoka 8-1, Ibaraki, Osaka 567-0047, Japan, and Department of Chemistry, Faculty of Science, National Taiwan University, Taipei, Taiwan

majima@sanken.osaka-u.ac.jp

Received April 1, 2005

Emission during the pulse radiolysis of **PE** in Bz

$$Bz \rightarrow e^-_S + Bz^{\bullet+}$$
$$e^-_S + PE \rightarrow PE^{\bullet-}$$
$$Bz^{\bullet+} + PE \rightarrow Bz + PE^{\bullet+}$$
$$PE^{\bullet+} + PE^{\bullet-} \rightarrow {}^1PE^* + PE$$
$$PE^{\bullet+} + PE^{\bullet-} \rightarrow {}^1PE_2^*$$
$$\left.\right\} \; 1_{a\text{-}e}$$
$$PE^{\bullet+} + PE^{\bullet-} \rightarrow {}^3PE^* + PE$$
$${}^3PE^* + {}^3PE^* \rightarrow {}^1PE^* + PE$$
$${}^3PE^* + {}^3PE^* \rightarrow {}^1PE_2^*$$
$$\left.\right\} \; 2_{c,f}$$
$${}^1PE^* \rightarrow PE + h\nu'$$
$${}^1PE_2^* \rightarrow 2\,PE + h\nu''$$

PE

R = H (**a**), Me (**b**), OMe (**c**), OCH(Me)$_2$ (**d**), NMe$_2$ (**e**), NEt$_2$ (**f**)

Efficient monomer and excimer emission from various donor−acceptor substituted phenylethynes (**PE**), which are known as efficient electrogenerated chemiluminescent molecules, was observed with time-resolved fluorescence measurement during the pulse radiolysis in benzene. On the basis of the transient absorption and emission measurements, and steady-state measurements, the formation of **PE** in the singlet excited state (^{1}**PE***) and the excimer (^{1}**PE**$_2$*) can be interpreted by the charge recombination between the **PE** radical cation (**PE**$^{\bullet+}$) and the **PE** radical anion (**PE**$^{\bullet-}$) which are generated initially from the radiolytic reaction in benzene. It is suggested that the positive and negative charges are localized on the donor and acceptor moieties in the radical cation and anion, respectively. This mechanism is reasonably explained by the relationship between the annihilation enthalpy changes ($-\Delta H'°$) and singlet excitation energies of donor-substituted phenyl-(9-acridinyl)ethynes (**1**$_{a-e}$). In addition to the monomer emission, the compounds bearing weak donors (**1**$_{a-d}$) show the excimer emission due to a very small twist angle between the donor and acceptor moieties. For the phenyl(9-cyano-10-anthracenyl)ethynes (**2**$_c$ and **2**$_f$), although they also show the monomer and excimer emissions, it cannot be explained by the relationship between $-\Delta H'°$ values and their singlet excitation energies, suggesting the formation of the ICT state and H-type excimer in which two 9-cyano-10-anthracenyl moieties are stacked face-to-face with donor bearing a benzene ring projecting perpendicularly away from each other through the charge recombination between **2**$^{\bullet+}$ and **2**$^{\bullet-}$ and/or triplet−triplet annihilation.

Introduction

An extensive number of studies have been devoted to radical cations (**M**$^{\bullet+}$) and anions (**M**$^{\bullet-}$) generated from detachment and attachment of an electron from and to a neutral solute molecule (**M**), respectively. Organic radical ions are important intermediates in photoinduced electron-transfer reactions and radiation chemical reac-

tions, with attention being focused on their reactivities.[1] The formation and reaction of radical ions in solution have been investigated by various methods such as pulse radiolysis, laser flash photolysis, and electrochemical reaction.
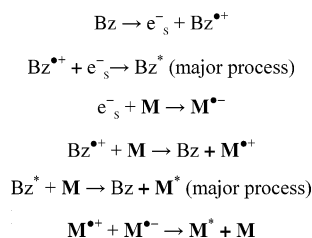
In the pulse radiolysis of solutions, the solvent molecules are initially ionized to give holes and electrons which react with the solute molecules. In nonpolar
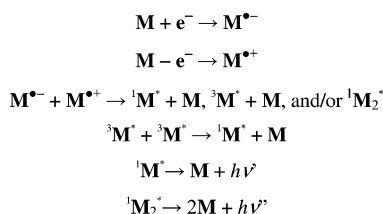
(1) (a) Fox, M. A.; Chanon, M. *Photoinduced Electron Transfer*; Elsevier: Amsterdam, The Netherlands, 1988. (b) Kavarnos, G. J.; Turro, N. J. *Chem. Rev.* **1986**, *86*, 401.

SCHEME 1. Pulse Radiolysis of M in Bz

$$Bz \rightarrow e^-_s + Bz^{\bullet+}$$

$$Bz^{\bullet+} + e^-_s \rightarrow Bz^* \text{ (major process)}$$

$$e^-_s + M \rightarrow M^{\bullet-}$$

$$Bz^{\bullet+} + M \rightarrow Bz + M^{\bullet+}$$

$$Bz^* + M \rightarrow Bz + M^* \text{ (major process)}$$

$$M^{\bullet+} + M^{\bullet-} \rightarrow M^* + M$$

SCHEME 2. Mechanism for the Electrogenerated Chemiluminescence (ECL)

$$M + e^- \rightarrow M^{\bullet-}$$

$$M - e^- \rightarrow M^{\bullet+}$$

$$M^{\bullet-} + M^{\bullet+} \rightarrow {}^1M^* + M, {}^3M^* + M, \text{ and/or } {}^1M_2^*$$

$$^3M^* + {}^3M^* \rightarrow {}^1M^* + M$$

$$^1M^* \rightarrow M + h\nu'$$

$$^1M_2^* \rightarrow 2M + h\nu''$$

solvents, hole and electron are initially formed and undergo partly the fast geminate charge recombination to give the solvent molecules in the singlet and triplet excited states. For example, initial products during the pulse radiolysis of benzene (Bz) are solvated electron (e^-_S), Bz radical cation ($Bz^{\bullet+}$), and Bz in the excited state (Bz^*) which react with **M** to give $M^{\bullet-}$, $M^{\bullet+}$, and **M** in the singlet and triplet excited states ($M^* = {}^1M^*$ and $^3M^*$), respectively, as shown in Scheme 1.[2] Usually M^* is the main product, while $M^{\bullet+}$ and $M^{\bullet-}$ are produced in minor yields. Therefore, the formation of M^* from the charge recombination between $M^{\bullet+}$ and $M^{\bullet-}$ is a minor process, and no $^1M^*$ and only a little $^3M^*$ exist at a few tens of nanoseconds after an electron pulse during the pulse radiolysis.

Radical ions are also formed by the electrochemical reaction in solution. Recently, various studies on the electrogenerated chemiluminescence (ECL)[3] have been reported to confirm the emissive species through the charge recombination between $M^{\bullet+}$ and $M^{\bullet-}$ in solution. ECL mainly results from $^1M^*$ and/or the singlet excimer of $^1M^*$ ($^1M_2^*$), as shown in Scheme 2. For pyrene, perylene, poly(9,9-dioctylfluorene), donor-substituted phenylquinolinylethynes, donor-substituted phenyl(9-acridinyl)ethynes, and phenyl(9-cyano-10-anthracenyl)ethynes, excimer type ECL was observed.[4−6] However, the selective formation of $^1M_2^*$ as the emissive species has not been fully understood.

(2) (a) Candeias, L. P.; Wilderman, J.; Hadziioannou, G.; Warman, J. M. *J. Phys. Chem. B* **2000**, *104*, 8366. (b) Candeias, L. P.; Grozema, F. C.; Padmanaban, G.; Ramakrishnan, S.; Siebbeles, L. D. A.; Warman, J. M. *J. Phys. Chem. B* **2003**, *107*, 1554. (c) Priyadarsini, K. I.; Mohan, H.; Birkett, P. R.; Mittal, J. P. *J. Phys. Chem.* **1996**, *100*, 501. (d) Seki, S.; Koizumi, Y.; Kawaguchi, T.; Habara, H.; Tagawa, S. *J. Am. Chem. Soc.* **2004**, *126*, 3521. (e) Grozema, F. C.; Hoofman, R. J. O. M.; Candeias, L. P.; de Haas, M. P.; Warman, J. M.; Siebbeles, L. D. A. *J. Phys. Chem. A* **2003**, *107*, 5976.

(3) (a) Faulkner, L. R.; Bard, A. J. *Electroanalytical Chemistry*; Marcel Dekker: New York, 1977; Vol. 10, pp 1−95. (b) Bard, A. J.; Faulkner, L. R. *Electrochemical Methods Fundamentals and Applications*, 2nd ed.; John Wiley and Sons: New York, 2001, pp 736−745. (c) Richter, M. M. *Chem. Rev.* **2004**, *104*, 3003.

(4) (a) Chandross, E. A.; Longworth, J. W.; Visco, R. E. *J. Am. Chem. Soc.* **1965**, *87*, 3259. (b) Lai, R. Y.; Fleming, J. J.; Merner, B. L.; Vermeij, R. J.; Bodwell, G. J.; Bard, A. J. *J. Phys. Chem. A* **2004**, *108*, 376. (c) Oyama, M.; Mitani, M.; Okazaki, S. *Electrochem. Commun.* **2000**, *2*, 363. (d) Prieto, I.; Teetsov, J.; Fox, M. A.; Vanden Bout, D. A.; Bard, A. J. *J. Phys. Chem. A* **2001**, *105*, 520.

SCHEME 3

R = H (a), Me (b), OMe (c), OCHMe₂ (d), NMe₂ (e), NEt₂ (f)
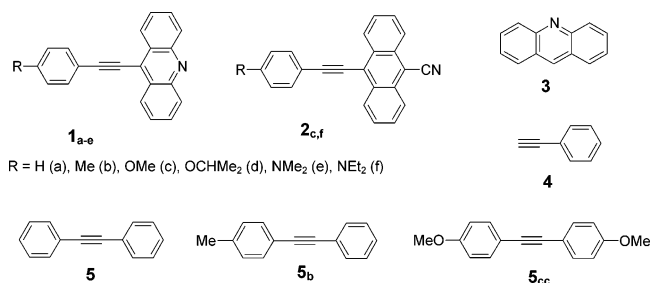
According to the ECL mechanism, when $M^{\bullet+}$ and $M^{\bullet-}$ are produced at sufficient concentrations, $^1M^*$, $^3M^*$, and/or $^1M_2^*$ can be generated from the charge recombination between $M^{\bullet+}$ and $M^{\bullet-}$ during the pulse radiolysis of the ECL molecules in Bz. We have previously reported that the efficient emissions during the pulse radiolysis of electrochemical luminescent substitute quinoline with donor−acceptor character (**PnQ**).[7] The emission was suggested to originated from the $^1PnQ^*$ generated from the charge recombination between $PnQ^{\bullet+}$ and $PnQ^{\bullet-}$ which are yielded from the initial radiolytic reaction in Bz.

In this paper, we report the observation of the efficient emission from the charge recombination between radical cations and radical anions of various donor−acceptor substituted phenylethynes (**PE**) such as donor-substituted phenyl(9-acridinyl)ethynes ($1_{a−e}$) and phenyl(9-cyano-10-anthracenyl)ethynes ($2_{c,f}$) during the pulse radiolysis of **PE** in Bz. In addition, the parent unsubstituted molecules of **PE**, acridine (**3**), and several phenylacetylene derivatives (**PA** = phenylacetylene (**4**), diphenylacetylene (**5**), 4-methyldiphenylacetylene (5_b), and 4,4′-dimethoxydiphenylacetylene (5_{cc})) were also examined for the emission measurement (Scheme 3). **PE** is known as the ECL molecule because **PE** in the singlet state ($^1PE^*$) and the emissive $^1PE^*$ excimer ($^1PE_2^*$) are generated from the triplet−triplet annihilation (T-route) of **PE** in the triplet excited state ($^3PE^*$).[6] Using the pulse radiolysis technique, both $PE^{\bullet+}$ and $PE^{\bullet-}$ can be generated at the same time in Bz. It is expected that $^1PE^*$, $^3PE^*$, and/or $^1PE_2^*$ can be generated from the charge recombination between $PE^{\bullet+}$ and $PE^{\bullet-}$ during the pulse radiolysis of **PE** in Bz, when $PE^{\bullet+}$ and $PE^{\bullet-}$ are produced at sufficient concentrations. Therefore, the emission mechanism of ECL molecules can be investigated in detail with the time-resolved transient absorption and emission measurement during the pulse radiolysis.

Results and Discussion

Emission Properties and Photophysical and Electrochemical Properties. The photophysical properties of **PE** (**1** and **2**), **3**, and **PA** (**4** and **5**) in acetonitrile and in Bz are listed in Table 1, together with the electrochemical properties in acetonitrile. Except for amino-

(5) (a) Elangovan, A.; Chen, T.-Y.; Chen, C.-Y.; Ho, T.-I. *Chem. Commun.* **2003**, 2146. (b) Elangovan, A.; Yang, S.-W.; Lin, J.-H.; Kao, K.-M.; Ho, T.-I. *Org. Biomol. Chem.* **2004**, *2*, 1597.

(6) (a) Elangovan, A.; Chiu, H.-H.; Yang, S.-W.; Ho, T.-I. *Org. Biomol. Chem.* **2004**, *2*, 3113. (b) Elangovan, A.; Kao, K.-M.; Yang, S.-W.; Chen, Y.-L.; Ho, T.-I.; Su, Y. O. *J. Org. Chem.* **2005**, 70, 4460.

(7) Samori, S.; Hara, M.; Tojo, S.; Fujitsuka, M.; Yang, S.-W.; Elangovan, A.; Ho, T.-I.; Majima, T. *J. Phys. Chem. B* **2005**, *109*, 11735.

TABLE 1. Photophysical and Electrochemical Properties of PE (1 and 2), 3, and PA (4 and 5)

	in CH$_3$CN			in Bz					in CH$_3$CN		
PE	λ_{max}^{Abs}/nm	λ_{max}^{Fl}/nm	$\lambda_{max}^{ECL\,b}$/nm	λ_{max}^{Abs}/nm	λ_{max}^{Fl}/nm	ϕ_{fl} ($\times 10^{-2}$)	τ_{fl}/ns	E_{S1}/eV	$E_{red}^{\,f}$/V	$E_{ox}^{\,f}$/V	$-\Delta H^{\circ}$/eV
1$_a$	417	431	473	398	433, 457	21	1.3	2.71	−0.86	1.66	2.36
1$_b$	419	434	482	401	434, 460	33	1.6	2.70	−0.85	1.67	2.36
1$_c$	422	464	480	404	440, 465	65	2.0	2.67	−0.80	1.64	2.28
1$_d$	424	469	487	406	443, 467	73	2.1	2.66	−0.86	1.53	2.23
1$_e$	446	569	534	450	515	71	2.5	2.41	−0.84	0.98	1.66
2$_c$	448	496	536	431	474, 499	73	3.1	2.48	−0.89	1.49	2.22
2$_f$	488^a	604^a	550	490	554	44	3.1	2.24	−0.90	0.87	1.61
3	356	446	c	358	410	0.33^d	0.054^d	3.02	−2.1^g	1.29^g	3.23
4	270	317	c	319	393	11	2.2	3.16	−2.81^h	1.96^i	4.61
5	279	331	520	280	402	3.8	e	3.08	−2.53^h−2.8(2nd)	1.52^j	3.89, 4.16
5$_b$	326	420	c	300	372	0.017	e	3.33	−2.45^k	1.84	4.13
5$_{cc}$	312	333	c	279	374	2.3	e	3.32	−2.2	0.88^l	2.92

^{a} In dichloromethane. ^{b} Reference 6. ^{c} No ECL was observed. ^{d} Reference 8. ^{e} Not determined. ^{f} Potential is estimated vs Ag/Ag$^+$. ^{g} Reference 10a. ^{h} In *N,N*-dimethylformamide, ref 10b. ^{i} Reference 10c. ^{j} Reference 10d. ^{k} In *N,N*-dimethylformamide, ref 10e. ^{l} Reference 10f.
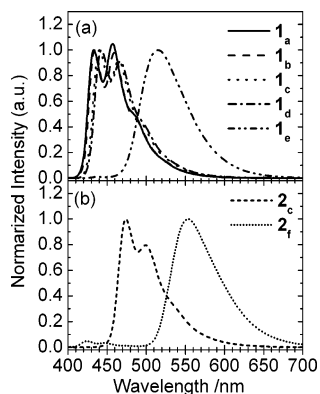

FIGURE 1. Fluorescence spectra measured by the steady-state measurement of **PE** (**1** (a) and **2** (b)) in Ar-saturated Bz.

substituted **PE** (**1$_e$** and **2$_f$**), two fluorescence peaks were observed for **PE**. The fluorescence quantum yields (ϕ_{fl}) were determined from the integration of the fluorescence using an external standard of **3** in Ar-saturated Bz (ϕ_{fl} = 3.3 × 10^{-3}).[8] The excitation energies of the lowest singlet excited state (E_{S1}) were estimated from the peak wavelengths of the fluorescence spectra. The ground-state absorption peaks of **PE** in Bz and acetonitrile were observed at 417−490 nm with a little influence of the solvent polarity. The fluorescence peaks in Bz were observed at 433−554 nm (Figure 1), while those in acetonitrile were at 431−569 nm with a red-shift due to the high solvent polarity. **2$_f$** did not fluoresce in acetonitrile but showed emission with a peak at 604 nm in dichloromethane. Using a setup consisting of a fluorescence spectrophotometer and a voltammetric instrument with a PC interface, we observed ECL emission of **PE** (1−10 mM) at 470−550 nm in acetonitrile with 0.05 M tetrabutylammonium perchlorate (TBAP) as the supporting electrolyte. These results are explained by the annihilation enthalpy change ($-\Delta H^{\circ}$) for the charge recombination between **M$^{\bullet+}$** and **M$^{\bullet-}$** that yields the neutral reactant precursor molecules in their ground states, as expressed by eq 1,[6,9]

$$-\Delta H^{\circ} = E_{ox} - E_{red} - 0.16 \text{ eV} \qquad (1)$$

where E_{ox} and E_{red} are the oxidation and reduction potentials of **M** in acetonitrile solution, respectively.

Thus, the standard potentials for the half reactions can be reliably estimated from cyclic voltammetric peak potentials in acetonitrile solution. The additional term (−0.16 eV) in eq 1 is due to the difference between their voltammetric peak potentials and their standard potentials (0.06 eV) and the $T\Delta S^{\circ}$ term (0.1 eV).

The calculated $-\Delta H^{\circ}$ values for **PE** are listed in Table 1. The charge recombination between **M$^{\bullet+}$** and **M$^{\bullet-}$** occurs when $-\Delta H^{\circ}$ values (eq 1) are higher than their E_{S1} (Table 1). However, this relation can be applied only when the singlet excited state was directly formed through the charge recombination between **M$^{\bullet+}$** and **M$^{\bullet-}$**. In the case of **PE**, it is assumed that ^{3}**PE*** is generated and followed by the triplet−triplet annihilation giving ^{1}**PE$_2$***, leading to the ECL (T-route).[6] In the emissions generated through the T-route, the energy from the triplet−triplet annihilation must be pooled to be sufficient for the formation of the singlet excited state. Some monomer and excimer emissions cannot be explained by eq 1 because ^{1}**PE$_2$*** is generated through the T-route. The absorption and fluorescence peaks of **1** in Bz were observed at 398−450 and 433−515 nm, respectively (Figure 1a and Table 1). It was shown that both absorption and fluorescence peaks shifted to longer wavelength with an increase of the electron-donating character of the substituent. This tendency is also observed for **2** (Figure 1b and Table 1). The broad and very weak emission of **3** was observed at a longer wavelength, and assigned to the excimer emission. The ϕ_{fl} values of **PE** except for **2$_f$** increased with an increase of the fluorescence lifetime (τ_{fl}), suggesting the lifetime of the S$_1$ state governs ϕ_{fl}. It is assumed that the longer τ_{fl} value for ^{1}**PE*** bearing strong donors (**1$_e$**, **2$_c$**, and **2$_f$**) results from the formation of the singlet intramolecular charge transfer (ICT) state with the larger twisted angle between the donor and acceptor moieties.[6]

Emission Spectra Observed during the Pulse Radiolysis of PE in Bz. The time-resolved emission spectra were observed to show monotonic decay in the 40-ns time scale after an electron pulse during the pulse radiolysis of **PE** in Ar-saturated Bz (Figures 2 and 3). It should be noted that all **PE** show emissions with peaks at 457−618 nm in the 40-ns time scale after an electron

(8) Diverdi, L. A.; Topp, M. R. *J. Phys. Chem.* **1984**, *88*, 3447.
(9) (a) Weller, A.; Zachariasse, K. *J. Chem. Phys.* **1967**, *46*, 4984. (b) Faulkner, L. R.; Tachikawa, H.; Bard, A. *J. Am. Chem. Soc.* **1972**, *94*, 691.
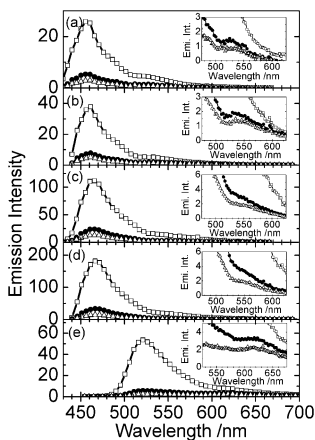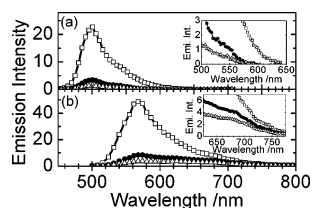
FIGURE 2. Emission spectra recorded at time $t = 10$ (open square), 20 (solid circle), and 30 (open triangle) ns after an electron pulse during the pulse radiolysis of 1_a (a), 1_b (b), 1_c (c), 1_d (d), and 1_e (e) in Ar-saturated Bz. Inset: Expanded spectra in the longer wavelength region.

FIGURE 3. Emission spectra recorded at time $t = 10$ (open square), 20 (solid circle), and 30 (open triangle) ns after an electron pulse during the pulse radiolysis of 2_c (a) and 2_f (b) in Ar-saturated Bz. Inset: Expanded spectra in the longer wavelength region.

pulse during the pulse radiolysis. For 1_a, 1_b, and 1_e, a new emission peak was observed at a longer wavelength during the pulse radiolysis (Figures 2 and 3, inset), although this was not observed in the steady-state measurement (Figure 1). It can be assigned to be excimer emission. For 1_c, 1_d, and 2, a weak and broad emission peak assigned to the excimer emission was also observed at a longer wavelength. In addition, compared to the fluorescence spectra observed in the steady-state measurement, the shape of the emission spectra was changed and only one emission peak was observed around 460–470 nm during the pulse radiolysis. The disappearance of the emission peak around 430 nm is due to the self-absorption as a result of the high concentrations of **PE**. It is confirmed at high concentration (5 mM) that **PE** shows the emission spectra with peaks at 457–574 nm in the steady-state measurement. In contrast to **PE**, very weak emissions from **3** and **PA** were observed during the pulse radiolysis. The emission spectral data of **PE, 3**, and **PA** obtained during the pulse radiolysis are summarized in Table 2. The relative emission intensity was determined from the integration of the emission spectrum observed at 10 ns after an electron pulse during the pulse radiolysis. The donor moiety of **PE** is toluene or anisole auxochrome with a fluorescence peak at 280–300 nm, while the acceptor moiety of **PE** is **3** with a fluorescence peak at 410 nm. Therefore, the emission of **PE** corresponds to the acceptor moiety, **3**.

According to the $-\Delta H°$ values (Table 2), **PE** emits light because $^1\mathbf{PE}^*$ are generated via the T-route in the

TABLE 2. Emission Peak (λ_{max}^{Em}) and Relative Emission Intensity of PE (1 and 2), 3, and PA (4 and 5) Observed at 10 ns after an Electron Pulse during the Pulse Radiolysis in Bz, Together with the ECL Emission Peak and Intensity in Acetonitrile

PE	λ_{max}^{Em}/nm	rel emission intensity[a] (%)	λ_{max}^{ECL}/nm	ECL intensity[d] (%)
1_a	457, 527	21	473	4.4
1_b	461, 534	27	482	2.2
1_c	467, 550[b]	92	480	9.0
1_d	468, 570[b]	140	487	1.2
1_e	525, 618	54	534	2.1
2_c	500, 545[b]	18	536	20
2_f	574, 680[b]	62	550	12
3	410, 460	0.3	c	0
4	378	0.9	c	0
5	338, 467	2.1	520	7.0
5_b	422, 577	0.4	c	0
5_{cc}	335, 507	4.0	c	0

[a] Relative to the intensity for 2-(*p*-methoxyphenylethynyl)quinoline = 100%.[7] Emission intensity was obtained by integration of emission observed at all wavelengths at 10 ns after the electron pulse irradiation. [b] Broad peak. [c] No or very weak emission was observed. [d] Reference 6. Relative to the ECL intensity of tris(2,2′-bipyridyl)ruthenium(II)oxalate complex = 100%.

electrochemical reactions.[6] However, compared to the ECL intensity, **PE** showed strong fluorescence during the pulse radiolysis in Bz (Table 2). In particular, 1_d showed the highest fluorescence intensity (140) during the pulse radiolysis, in contrast to the lowest ECL intensity (1.2) among **PE**. Therefore, the occurrence of the efficient emission during the pulse radiolysis of **PE** corresponds to a mechanism different from the T-route mechanism.

The emission intensities of **PE** observed during the pulse radiolysis were much higher than those of **3** and the corresponding **PA**. For example, the emission intensity of 1_b was 66 times higher than that of 5_b. Similarly, that of 1_c was 23 times higher than that of 5_{cc}. These results indicate that strong electronic coupling between the donor and acceptor is responsible for the efficient emission during the pulse radiolysis of **PE** in Bz. In addition, it is noteworthy that, although the ϕ_{fl} value of 2_c (0.73) is higher than that of 1_c (0.65), the emission intensity of 2_c during the pulse radiolysis (18) is lower than that of 1_c (92). Compared with 2_c, although the ϕ_{fl} value of 2_f is low (0.44), the emission intensity of 2_f during the pulse radiolysis is shown to be high (62). For 2_f, the emission was observed with an extremely long lifetime because of the delayed fluorescence. However, the intensity of this delayed fluorescence observed during the pulse radiolysis was too weak. The same delayed fluorescence was also observed during the laser flash photolysis, as described later.

The emission behavior was investigated by changing the concentration of 1_a (1, 5, and 10 mM) in Bz during the pulse radiolysis. In the steady-state measurement, the fluorescence spectra showed no excimer emissions at these concentrations. Figure 4 shows the emission spectra of 1_a in Bz during the pulse radiolysis. The intensities were normalized to the emission peak intensity at 457 nm for three spectra. The emission intensity observed at 527 nm increased with an increase in the concentration, suggesting that the emission is assigned to the excimer. At 5 mM, the emission lifetimes at 457 and 550 nm were approximately 10 ns (Figure 4, inset). It is
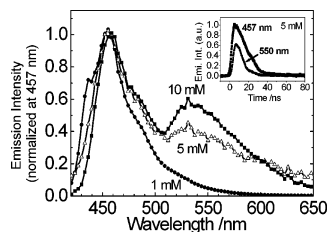
FIGURE 4. Emission spectra recorded at time $t = 30$ ns after an electron pulse during the pulse radiolysis of 1_a (1, 5, and 10 mM) in Ar-saturated Bz. Inset: Time profiles of the transient absorptions at 457 and 550 nm at 5 mM of 1_a.
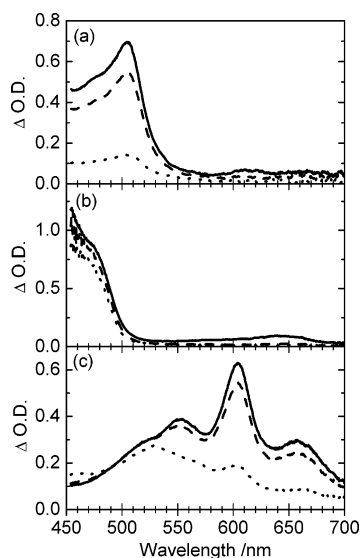

FIGURE 5. Transient absorption spectra observed at time $t = 100$ ns (solid line), 1 (broken line), and 10 μs (dotted line) after an electron pulse (8 ns) during the pulse radiolysis of 1_a (5 mM) in Ar-saturated Bz (a), DCE (b), and DMF (c).

suggested that the monomer and excimer lifetimes are governed by the same precursor, which converts the monomer and excimer through the same reaction process.

Transient Absorption Spectra Observed during the Pulse Radiolysis of PE. To generate both $PE^{\bullet+}$ and $PE^{\bullet-}$ and to observe the annihilation of $PE^{\bullet+}$ and $PE^{\bullet-}$ through the charge recombination, Bz was used as solvent for the pulse radiolysis of **PE**. Figure 5a shows the transient absorption spectra observed during the pulse radiolysis of 1_a in Ar-saturated Bz. The transient absorption spectra of $Bz^{\bullet+}$ and Bz^* have been reported to have a peak at 400 and 235 nm with a very low molar absorption coefficient.[7,11] It is assumed that e^-_S is rapidly trapped by 1_a or undergoes fast geminate charge recombination. Therefore, e^-_S cannot be observed under the present experimental conditions. The transient absorption spectrum observed at $t = 50$ ns after an electron pulse in Figure 5a can be assigned to $1_a^{\bullet+}$, $1_a^{\bullet-}$, and/or $^3 1_a^*$.

TABLE 3. Transient Absorption Peaks (λ_{max}) and Half Lifetimes ($\tau_{1/2}$) Observed during the Pulse Radiolysis of PE in Ar-Saturated Bz, DCE, and DMF

	in Bz		in DCE		in DMF	
PE	λ_{max}/nm	$\tau_{1/2}/\mu$s	λ_{max}/nm	$\tau_{1/2}/\mu$s	λ_{max}/nm	$\tau_{1/2}/\mu$s
1_a	505	2.9	642	0.21	553, 604, 656	3.4
1_b	512	2.1	658	0.17	555, 604, 653	2.0
1_c	524	2.3	608, 664	0.19	554, 600, 648	2.5
1_d	528	2.1	613, 662	0.31	559, 599, 656	3.4
1_e	591	2.0	650–750	0.15	600, 653	3.8
2_c	515	3.5	651, 716	1.0	650, 728	28
2_f	600	2.0	a	a	a	a

^{a} Not determined.

To confirm the transient absorption spectra of $1_a^{\bullet+}$ and $1_a^{\bullet-}$, the pulse radiolysis of 1_a in Ar-saturated DCE and DMF was also examined. It is established that $M^{\bullet+}$ is generated during the pulse radiolysis of **M** in DCE,[12] while $M^{\bullet-}$ is in DMF.[13] Figure 5b shows the transient absorption observed during the pulse radiolysis of 1_a in Ar-saturated DCE. Although a broad peak at 642 nm disappeared, that around 450 nm remained even in the time scale longer than 10 μs. Therefore, the absorption peak around 450–500 nm is assumed to be that of a stable product, while the peak observed at 642 nm ($\tau_{1/2}$ = 210 ns) is assigned to the radical cation of 1_a ($1_a^{\bullet+}$). It seems that Cl^- reacts with $1_a^{\bullet+}$ to give the product having an absorption peak around 450–500 nm.[7] For **AD** in Ar-saturated DCE, two transient absorption peaks observed around 400–430 nm remained even in the time scale longer than 10 μs, and at 464 nm with $\tau_{1/2}$ = 86 ns. The long-lived one observed around 400–430 nm is also assigned to a stable product. The peak at 464 nm is reasonably assigned to $AD^{\bullet+}$.[14]

Figure 5c shows the transient absorption observed during the pulse radiolysis of 1_a in Ar-saturated DMF. The peak observed at 553, 604, and 656 nm ($\tau_{1/2}$ = 3.4 μs) is assigned to the radical anion of 1_a ($1_a^{\bullet-}$). At 10 μs, the new emission peak was observed at 528 nm. It seems that $1_a^{\bullet-}$ reacts to give a product having an absorption peak at 528 nm. Similarly, the transient absorption spectra assigned to $1_a^{\bullet+}$ and $1_a^{\bullet-}$ were observed during the pulse radiolysis of other **PE** in DCE and DMF, respectively. These results are summarized in Table 3. In Bz solution, the transient absorptions of $PE^{\bullet+}$ and $PE^{\bullet-}$ were not observed. Therefore, it is assumed that $PE^{\bullet+}$ and $PE^{\bullet-}$ immediately recombine to give $^1PE^*$, $^3PE^*$, and $^1PE_2^*$ within a pulse duration.[7]

Emission and Absorption Spectra Observed during the Laser Flash Photolysis of PE in Bz. To assign the transient species in detail, the transient absorption spectra of **PE** in Bz were measured during the 355-nm

(10) (a) Wilkinson, F.; Tsiamis, C. *J. Am. Chem. Soc.* **1983**, *105*, 767. (b) Wawzonek, S.; Wearring, D.; *J. Am. Chem. Soc.* **1959**, *81*, 2067. (c) Katz, M.; Riemenschneider, P.; Wendt, H. *Electrochim. Acta* **1972**, *17*, 1895. (d) Marcoux, L.; Adams, R. N. *J. Electroanal. Chem.* **1974**, *49*, 111. (e) Sioda, R. E.; Cowan, D. O.; Koski, W. S. *J. Am. Chem. Soc.* **1967**, *89*, 230. (f) Carious, M. *Tetrahedron* **1991**, *47*, 799.

(11) (a) Mohan, H.; Mittal, J. P. *J. Phys. Chem. A* **1999**, *103*, 379. (b) Carmichael, I.; Helman, W. P. *J. Phys. Chem. Ref. Data* **1987**, *16*, 239.

(12) (a) Shida, T.; Hamill, W. H. *J. Chem. Phys.* **1966**, *44*, 2369, 2375, 3472. (b) Shida, T.; Kato, T. *Chem. Phys. Lett.* **1979**, *68*, 106. (c) Grimison, A.; Simpson, G. A. *J. Phys. Chem.* **1968**, *72*, 1776. (d) Ishida, A.; Fukui, M.; Ogawa, H.; Tojo, S.; Majima, T.; Takamuku, S. *J. Phys. Chem.* **1995**, *99*, 10808. (e) Majima, T.; Tojo, S.; Ishida, A.; Takamuku, S. *J. Org. Chem.* **1996**, *61*, 7793. (f) Majima, T.; Tojo, S.; Ishida, A.; Takamuku, S. *J. Phys. Chem.* **1996**, *100*, 13615.

(13) (a) Honda, E.; Tokuda, M.; Yoshida, H.; Ogasawara, M. *Bull. Chem. Soc. Jpn.* **1987**, *60*, 851. (b) Huddleston, R. K.; Miller, J. R. *J. Phys. Chem.* **1982**, *86*, 2410. (c) Majima, T.; Fukui, M.; Ishida, A.; Takamuku, S. *J. Phys. Chem.* **1996**, *100*, 8913. (d) Majima T.; Tojo, S.; Takamuku, S. *J. Phys. Chem. A* **1997**, *101*, 1048.

(14) Shiba, T. *Electronic Absorption Spectra of Radical Ions*; Elsevier: Amsterdam, The Netherlands, 1988.
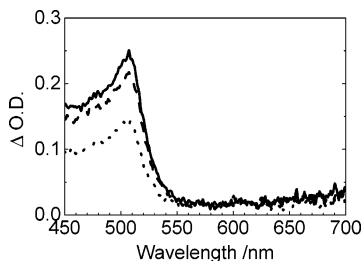
FIGURE 6. Time-resolved transient absorption spectra observed at time $t = 4$ (solid line), 5 (broken line), and 10 (dotted line) μs after a laser pulse during the laser flash photolysis of 1_a (20 μM) in Ar-saturated Bz.

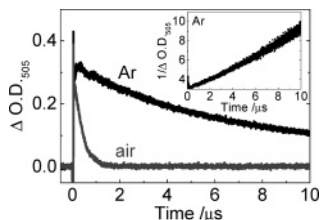**FIGURE 7.** Time profiles of transient absorption at 505 nm observed during the laser flash photolysis of 1_a (20 μM) in Ar- and air-saturated Bz. Inset: Time profile of ΔOD_{505}^{-1} in Ar-saturated Bz.

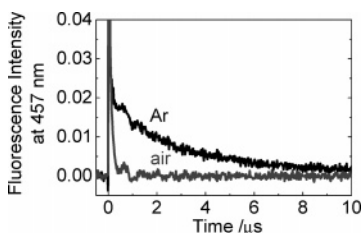**FIGURE 8.** Time profiles of emission at 457 nm observed during the laser flash photolysis of 1_a (20 μM) with Ar- and air-saturated Bz.

5-ns laser flash photolysis (Supporting Information, Figure S4). A transient absorption spectrum with a peak at 505 nm was observed during the laser flash photolysis of 1_a in Ar-saturated Bz (Figure 6). During the laser flash photolysis under the one-photon excitation condition, the most probable long-lived transient is $^3 1_a{}^*$, which is generated from intersystem crossing of $^1 1_a{}^*$. Therefore, the transient absorption spectrum, observed during the pulse radiolysis of 1_a in Ar-saturated Bz, is also assigned to mainly $^3 1_a{}^*$.

Figure 7 shows the time profiles of the transient absorption at 505 nm in Ar- and air-saturated Bz. In air-saturated condition, the transient absorption was immediately quenched by oxygen through the triplet energy transfer quenching mechanism. Therefore, the absorption with a peak at 505 nm is assigned to $^3 1^*$.[7]

Emission spectra of 1_a were also measured during the laser flash photolysis. Emissions with extremely long lifetimes (μs time scale) were observed for 1_a (Figure 8). Under air-saturated condition, the long-lived emission was also quenched by oxygen, suggesting that the emission originated from $^3 1_a{}^*$. The time profile of ΔOD_{505}^{-1} shows the decay of $^3 1_a{}^*$ obeys second-order kinetics (Figure 7, inset). These results suggest that the long lifetime emission corresponds to the "P-type" delayed

fluorescence of $^1 1_a{}^*$ generated from the triplet−triplet annihilation.[7,15] Similarly, the "P-type" delayed fluorescence was observed during the laser flash photolysis of other **PE** in Bz (Figure S5, Supporting Information). On the other hand, very weak "P-type" delayed fluorescence was observed during the pulse radiolysis of **PE** in Bz. Therefore, it is expected that $^1\mathbf{PE}^*$ and $^1\mathbf{PE_2}^*$ are mainly generated from the charge recombination between $\mathbf{PE}^{\bullet+}$ and $\mathbf{PE}^{\bullet-}$ during the pulse radiolysis.

Emission Mechanism. Because the efficient emission of **PE** during the pulse radiolysis seems to result from the donor−acceptor structure of **PE**, the characteristic emission mechanism for the donor−acceptor molecules should be involved. We have previously reported that the efficient emission was observed during the pulse radiolysis of **PnQ** with strong electric coupling between donor and acceptor through conjugation.[7]

It is suggested that the positive charge and negative charges in $\mathbf{PnQ}^{\bullet+}$ and $\mathbf{PnQ}^{\bullet-}$ are localized on the donor and acceptor moieties, respectively. It is also suggested for **PE** that negative charge is localized on the electron acceptor moiety in the radical anion (A$^{\bullet-}$−D), while positive charge is localized on the electron donor moiety in the radical cation (A−D$^{\bullet+}$). This scheme reasonably explains the emission mechanism during the pulse radiolysis of **1** in Bz. For 1_a, the E_{ox} value of the donor moiety (corresponding to benzene) is 2.08 V, while the E_{red} value of the acceptor moiety (corresponding to **AD**) is −2.1 V. Therefore, the $-\Delta H'^{\circ}$ value for the charge recombination between $1_a{}^{\bullet+}$ and $1_a{}^{\bullet-}$ with localized charges can be estimated to be 4.02 eV, which is sufficiently larger than the E_{S1} value. Similarly, the $-\Delta H'^{\circ}$ values for 1_b, 1_c, and 1_e are sufficiently larger than the E_{S1} values (Table 4). Therefore, it is suggested that the charge recombination between A$^{\bullet-}$−D and A−D$^{\bullet+}$ occurs to give $^1 1_{a-e}{}^*$ and $^1(1_{a-e})_2{}^*$ during the pulse radiolysis of 1_{a-e} in Bz (Scheme 4). The formation of $^1(1_{a-d})_2{}^*$ can be explained by the planar structure of 1_{a-d} and $^1 1_{a-d}{}^*$ in which the π-donor and π-acceptor moieties exist in the same plane because of the weak donor moiety. The compounds bearing weak donors (1_{a-d}) show excimer emission due to a very small twist angle between the donor and acceptor moieties.

For **2** their $-\Delta H'^{\circ}$ values are not sufficient to populate $^1 2^*$. This results in the lower emission intensity of 2_c during the pulse radiolysis, although it shows strong fluorescence in the steady-state measurement. For **PE** bearing strong donors (1_e, 2_c, and 2_f), the emissive singlet intramolecular charge transfer (ICT) state ($^1(\mathrm{A}^{\bullet-}-\mathrm{D}^{\bullet+})^*$) with the larger twisted angle is assumed.[6,17] The ICT states for 1_e, 2_c, and 2_f are also expected by their slightly longer τ_{fl} than those of other **PE** (Table 1).

The emission mechanism during the pulse radiolysis of **PE** can be divided into two categories. For 1_{a-d} with

(15) (a) Liu, D. K. K.; Faulkner, L. R *J. Am. Chem. Soc.* **1977**, *99*, 4594. (b) Bohne, C.; Abuin, E. B.; Scaiano, J. C. *J. Am. Chem. Soc.* **1990**, *112*, 4226.
(16) (a) Neikam, W. C.; Desmond, M. M. *J. Am. Chem. Soc.* **1964**, *86*, 4811. (b) Eberson, L. *J. Am. Chem. Soc.* **1967**, *89*, 4669. (c) Totah, R. A.; Hanzlik, R. P. *Biochemistry* **2004**, *43*, 7907. (d) Dileesh, S.; Gopidas, K. R. *J. Photochem. Photobiol. A* **2004**, *162*, 115. (e) Lewis, F. D.; Bedell, A. M.; Dykstra, R. E.; Elbert, J. E.; Gould, I. R.; Farid S. *J. Am. Chem. Soc.* **1990**, *112*, 8055.
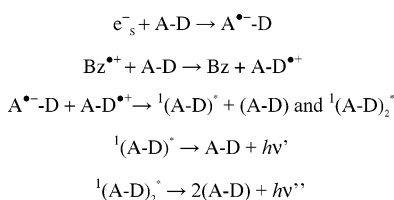(17) Fungo, F.; Wong, K.-T.; Ku, S.-Y.; Hung, Y.-Y.; Bard, A. J. *J. Phys. Chem. B* **2005**, *109*, 3984.

TABLE 4. Oxidation Potentials (E_{ox}) of Donor Moiety, Reduction Potentials (E_{red}) of Acceptor Moiety, Estimated Annihilation Enthalpy Values ($-\Delta H'^{\circ}$), and E_{S1} of PE

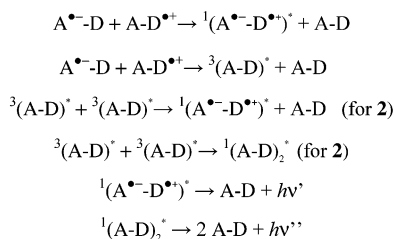|	in CH$_3$CN		in CH$_3$CN			in Bz
PE	donor	$E_{ox}{}^a$/V	acceptor	$E_{red}{}^a$/V	$-\Delta H'^{\circ}$/eV	E_{S1}/eV
1$_a$	benzene	2.08^b	acridine	−2.1^g	4.02	2.71
1$_b$	toluene	1.98^{b,c}	acridine	−2.1	3.92	2.70
1$_c$	anisole	1.35^c	acridine	−2.1	3.29	2.67
1$_d$	isopropoxybenzene	d	acridine	−2.1	-	2.66
1$_e$	N,N-dimethylaniline	0.55^e	acridine	−2.1	2.49	2.41
2$_c$	anisole	1.35^c	9-cyanoanthracene	−0.98^h	2.17	2.48
2$_f$	N,N-diethylaniline	0.47^f	9-cyanoanthracene	−0.98	1.29	2.24

^{a} Potential is estimated vs Ag/Ag$^+$. ^{b} Reference 16a. ^{c} Reference 16b. ^{d} Not determined. ^{e} Reference 16c. ^{f} Reference 16d. ^{g} Reference 8. ^{h} Reference 16e.

SCHEME 4. Mechanism of the Emission during the Pulse Radiolysis of 1$_{a-d}$ in Bz^a

$$e^-{}_s + A\text{-}D \rightarrow A^{\bullet-}\text{-}D$$

$$Bz^{\bullet+} + A\text{-}D \rightarrow Bz + A\text{-}D^{\bullet+}$$

$$A^{\bullet-}\text{-}D + A\text{-}D^{\bullet+} \rightarrow {}^1(A\text{-}D)^* + (A\text{-}D) \text{ and } {}^1(A\text{-}D)_2{}^*$$

$${}^1(A\text{-}D)^* \rightarrow A\text{-}D + h\nu'$$

$${}^1(A\text{-}D)_2{}^* \rightarrow 2(A\text{-}D) + h\nu''$$

^{a} 1$_{a-d}$ is shown as A−D where A and D are acridine and substituted benzenes, respectively.

**SCHEME 5. Mechanism of the Emission during the Pulse Radiolysis of 1$_e$, 2$_c$, and 2$_f$ in Bz^a**

$$A^{\bullet-}\text{-}D + A\text{-}D^{\bullet+} \rightarrow {}^1(A^{\bullet-}\text{-}D^{\bullet+})^* + A\text{-}D$$

$$A^{\bullet-}\text{-}D + A\text{-}D^{\bullet+} \rightarrow {}^3(A\text{-}D)^* + A\text{-}D$$

$${}^3(A\text{-}D)^* + {}^3(A\text{-}D)^* \rightarrow {}^1(A^{\bullet-}\text{-}D^{\bullet+})^* + A\text{-}D \quad \text{(for 2)}$$

$${}^3(A\text{-}D)^* + {}^3(A\text{-}D)^* \rightarrow {}^1(A\text{-}D)_2{}^* \quad \text{(for 2)}$$

$${}^1(A^{\bullet-}\text{-}D^{\bullet+})^* \rightarrow A\text{-}D + h\nu'$$

$${}^1(A\text{-}D)_2{}^* \rightarrow 2 A\text{-}D + h\nu''$$

^{a} 1$_e$, 2$_c$, and 2$_f$ are shown as A−D where A and D are **AD** or 9-cyanoanthracene and substituted benzenes, respectively. $^1(A^{\bullet-}-D^{\bullet+})^*$ and $^1(A-D)_2{}^*$ are assumed to be generated through the triplet−triplet annihilation for 2$_c$ and 2$_f$.

no or weak electron donating substituents and no or a small twist angle between the donor and acceptor planes, it is less favorable to populate the emissive singlet ICT state. Because of the planar structure, $^1\mathbf{1_{a-d}}^*$ forms the excimer $^1(\mathbf{1_{a-d}})_2{}^*$ in part. For 1$_e$, 2$_c$, and 2$_f$ the emission mechanism is quite different from that for 1$_{a-d}$. It is suggested that the radical cation and anion collide neck-to-neck to generate the singlet ICT state ($^1(A^{\bullet-}-D^{\bullet+})^*$), triplet excited state $^3(A-D)^*$, or H-type excimer $^1(A-D)_2{}^*$ in which two 9-acridinyl or 9-cyano-10-anthracenyl moieties are stacked in the face-to-face structure with the donor-bearing benzene rings projecting perpendicularly away from each other (Schemes 5 and 6).[6] When the $-\Delta H'^{\circ}$ value was higher than E_{S1}, $^1(A^{\bullet-}-D^{\bullet+})^*$ can be directly formed through the charge recombination for 1$_e$. When the $-\Delta H'^{\circ}$ value was lower than E_{S1}, $^1(A^{\bullet-}-D^{\bullet+})^*$ must be formed through the triplet−triplet annihilation for 2$_c$ and 2$_f$. The very weak "P-type" delayed fluorescence was observed for 2$_f$ in Bz during the pulse radiolysis. In the laser flash photolysis, the "P-type" delayed fluorescence was observed for all **PE**. At 10 μs after a laser pulse, the delayed fluorescence of 2$_f$ remained, while that of 2$_c$ disappeared (Figures S5, f and g). It is suggested

that the triplet−triplet annihilation occurred more effectively for 2$_f$ than for 2$_c$. Therefore, the emission intensity of 2$_f$ was higher than that of 2$_c$ during the pulse radiolysis, although the ϕ_{fl} value of 2$_f$ was lower than that of 2$_c$. In addition, the emission intensity of 2$_f$ during the pulse radiolysis was higher than that of 1$_a$ or 1$_b$. This is because of the slightly longer lifetime of the formed ICT state. It is assumed that the H-type excimer is also formed for 1$_e$, 2$_c$, and 2$_f$. The formation of this H-type excimer is suggested to be derived from the charge recombination for 1$_e$ or triplet−triplet annihilation for 2.

Conclusions

Various donor−acceptor **PE** with an ethynyl linkage, which are known as very efficient ECL molecules by the electrochemical reaction, showed the efficient monomer and excimer emission during the pulse radiolysis in Bz. The emission is suggested to originate from ^{1}**PE*** generated from the charge recombination between **PE**$^{\bullet+}$ and **PE**$^{\bullet-}$ which yield from the initial radiolytic reaction in Bz. The emission intensities of **PE** observed at 10 ns after an electron pulse were 8.8−91 times higher than that of **5** during the pulse radiolysis. These results indicate that the efficient emission is due to the donor−acceptor character of **PE**. It is suggested that the positive and negative charges in **PE**$^{\bullet+}$ and **PE**$^{\bullet-}$ are localized on the donor (substituted benzenes) and acceptor (**3**) moieties, respectively. For **1**, the $-\Delta H'^{\circ}$ values (2.49−4.02 eV) estimated for the charge recombination between **PE**$^{\bullet+}$ and **PE**$^{\bullet-}$ with localized charges are estimated from E_{ox} of substituted benzenes and E_{red} of **3** to be sufficiently larger than E_{S1} of **PE** (2.41−2.71 eV). **1** with weak electron donating substitutents (1$_{a-d}$) show the excimer emission due to a very small twist angle between the donor and acceptor moieties. For **2** (2$_c$ and 2$_f$), although they also show monomer and excimer emissions, it cannot be explained by the $-\Delta H'^{\circ}$ (2.17 and 1.29 eV, respectively) and their singlet excitation energies (2.48 and 2.24 eV, respectively), suggesting the monomer emission is derived from the ICT state that is generated directly from the charge recombination or through the triplet−triplet annihilation. The excimer emission is assumed to be derived from the H-type excimer. The formation of the H-type excimer is suggested to be generated directly from the charge recombination or triplet−triplet annihilation. For 2$_f$, the emission intensity during the pulse radiolysis was observed to be higher than that of 2$_c$, suggesting the

SCHEME 6. Proposed Structure for the Formation of the ICT State or *H*-Type Excimer during the Pulse Radiolysis of 2_f in Bz
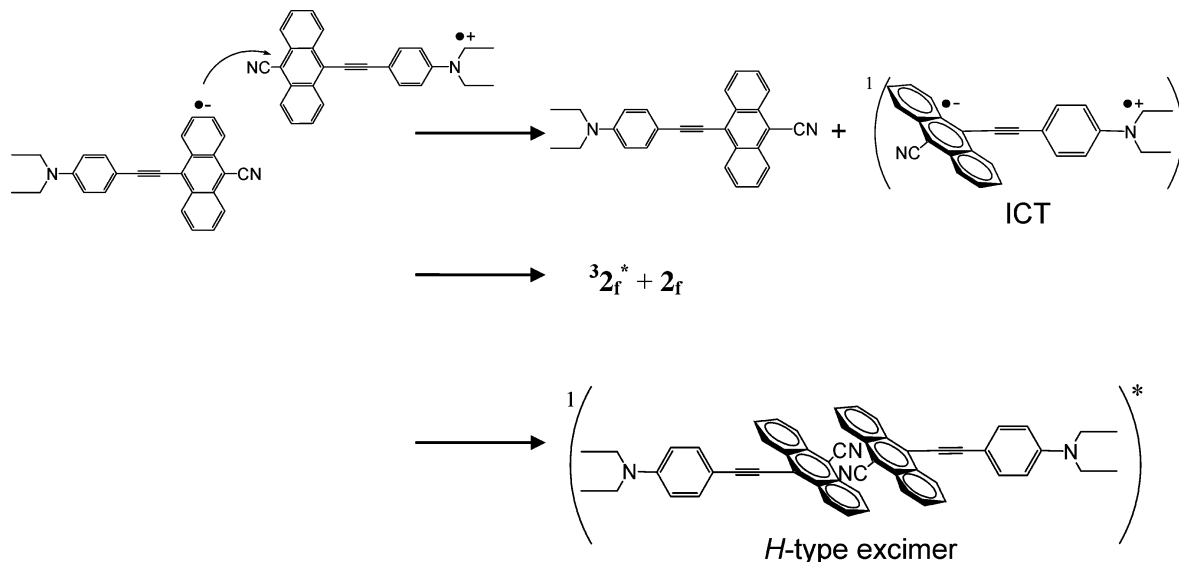
Experimental Section

Materials. 1_{a-e} and $2_{c,f}$ were synthesized respectively by cross-coupling of 9-chloroacridine and 9-bromo-10-cyanoanthracene with corresponding donor-substituted phenylethynes under modified Sonogashira reactions, respectively.[6] Phenylacetylene (**4**) was used as received. Acridine (**3**) and diphenylacetylene (**5**) were recrystallized from ethanol before use. 5_b and 5_{cc} were synthesized from reactions of phenylacetylenylcopper and 4-methoxyphenylenylcopper, respectively, with the corresponding substituted iodobenzene in pyridine according to literature procedures,[18] and recrystallized from ethanol before use. Spectral grade benzene (Bz), 1,2-dichloroethane (DCE), and *N,N*-dimethylformamide (DMF) were used without further purification.

Steady-State Measurements. UV spectra were recorded in Bz with a UV/visible spectrometer, using a transparent rectangular cell made from quartz ($1.0 \times 1.0 \times 4.0$ cm^3, path length of 1.0 cm). Fluorescence spectra were measured with a spectrofluorometer.

Pulse Radiolysis. Except for 1_e and 2_f, all the sample solutions were prepared in a 5 mM concentration in Bz, DCE, and DMF in a rectangular quartz cell ($0.5 \times 1.0 \times 4.0$ cm^3, path length of 1.0 cm). The solutions of 5 mM 1_e and 2_f were not prepared in Bz and DCE due to their poor solubility. Therefore, they were prepared in saturated concentrations (0.01−0.1 mM) in these solvents. These solutions were saturated with Ar gas by bubbling with it for 10 min at room temperature before irradiation. Pulse radiolysis was performed, as described previously,[7,19] using an electron pulse (28 MeV, 8 ns, 0.7 kGy) from an L-band linear accelerator at SANKEN, Osaka University.

Laser Flash Photolysis. Laser flash photolysis experiments were also carried out, as described previously,[7] using the third harmonic oscillation (355 nm) of a nanosecond Nd^{3+}:YAG laser (5-ns fwhm, 10 mJ pulse^{-1}) as an excitation source. Ar- and air-saturated Bz solutions were contained in a transparent rectangular quartz cell ($1.0 \times 1.0 \times 4.0$ cm^3, path length of 1.0 cm) at room temperature. The concentration of **PE** was adjusted to have an absorbance of 1.0 at excitation wavelength (355 nm).

Fluorescence Lifetime Measurements. Fluorescence lifetimes were measured by the single photon counting method, as described previously,[7] using a streakscope equipped with a polychromator. In the presence of oxygen, **PE** showed the long lifetime emission corresponds to the "P-type" delayed fluorescence. In this measurement, therefore, **PE** were prepared in O$_2$-saturated Bz.

Supporting Information Available: Ground-state absorption spectra of **PE** in Ar-saturated Bz, transient absorption spectra observed during the pulse radiolyses of **3** and **PE** (5.0 mM) in Ar-saturated Bz, DCE, and DMF, transient absorption and emission spectra observed during the laser flash photolyses of **PE** (30−300 μM) in Ar-saturated Bz. This material is available free of charge via the Internet at http://pubs.acs.org.

JO0506377

(18) Stephens, R. D.; Castro, C. E. *J. Org. Chem.* **1963**, *28*, 3313.

(19) (a) Kawai, K.; Yoshida, H.; Takada, T.; Tojo, S.; Majima, T. *J. Phys. Chem. B* **2004**, *108*, 13547. (b) Takada, T.; Kawai, K.; Tojo, S.; Majima, T. *J. Phys. Chem. B* **2003**, *107*, 14052. (c) Hara, M.; Tojo, S.; Majima, T. *Chem. Phys. Lett.* **2004**, *387*, 283.